Article ID: 1006-8775(2020) 02-0137-13

Resonance Effect in Interaction Between South Asian Summer Monsoon and ENSO During 1958–2018

YUAN Shuai (袁 帅)[1, 2], XU Jian-jun (徐建军)[2, 3], CHAN J C L (陈仲良)[4], CHIU Long-sang (赵朗生)[5], PAN Yu-shan (潘裕山)[1, 2]

(1. College of Ocean and Meteorology, Guangdong Ocean University, Zhanjiang, Guangdong 524088 China; 2. South China Sea Institute of Marine Meteorology, Guangdong Ocean University, Zhanjiang, Guangdong 524088 China; 3. Southern Marine Science and Engineering Guangdong Laboratory (Zhanjiang), Zhanjiang, Guangdong 524088 China; 4. School of Energy and Environment, City University of Hong Kong, Hongkong 999077 China; 5. AOES, College of Science, George Mason University, Fairfax, Virginia 22030 USA)

Abstract: The study has shown that the shear component of the vertical integrated kinetic energy (K_s) over the box (40ºE−100ºE, 0−20ºN) can be used to measure the intensity of the South Asian summer monsoon (SASM). Based on its value averaged between June and August, the SASM can be divided into strong and weak monsoon episodes. Between 1958 and 2018, there existed 16 (16) strong (weak) monsoon episodes. Based on the calendar year, the relationship between the SASM and ENSO episodes can be grouped into six patterns: weak monsoon - El Niño (WM-EN), normal monsoon - El Niño (NM-EN), weak monsoon - non ENSO (WM-NE), strong monsoon - La Niña (SM-LN), normal monsoon - La Niña (NM-LN) and strong monsoon - non ENSO (SM-NE). Previous studies suggest that the WM-EN and SM-LN patterns reflect the correlated relationship between the SASM and El Niño/Southern Oscillation (ENSO) events. Therefore, we name these two strongly coupled categories WM-EN and SM-LN as the resonance effect. Two important circulations, i.e., Walker circulation (WC) and zonal Asian monsoon circulation (MC), in the vertical plane are found to be not always correlated. The MC is controlled by thermal gradients between the Asian landmass and the tropical Indian Ocean, while the WC associated with ENSO events is primarily the east-west thermal gradient between the tropical South Pacific and the tropical Indian Ocean. Furthermore, the gradient directions caused by different surface thermal conditions are different. The main factor for the resonance effect is the phenomenon that the symbols of SSTA in the tropical Indian Ocean and the equatorial eastern Pacific are the same, but are opposite to that of the SSTA near the maritime continent.

Key words: South Asian Summer Monsoon; ENSO; resonance effect; monsoon circulation; Walker circulation

CLC number: P4 **Document code:** A

https://doi.org/10.46267/j.1006-8775.2020.013

1 INTRODUCTION

Because of their strong climate signal, both the south Asian summer monsoon (SASM) and the El Niño/Southern Oscillation (ENSO) have received much attention. Many studies have shown that the SASM is associated with interannual variations in the tropical ocean-atmosphere system, and in particularly, ENSO events (e. g. Shukla and Paolino [1]; Xu and Chan [2]; Rajeevan and McPhaden [3]; Soman and Slingo [4]; Shi et al. [5]). Lots of scientific evidence have also suggested that the Asian monsoon may have a strong impact on the development of ENSO events (Webster and Yang [6]; Meehl [7]; Lau and Yang [8]; Kirtman and Shukla [9]; Kim and Lau [10]; Wu [11]; Li Y et al. [12]). Wu and Meng (1998) found that the Indo-monsoon zonal circulation over the equatorial Indian Ocean and the Walker circulation over the Pacific Ocean are coupled in a way much like a pair of gears operating over the equatorial Indian and Pacific (GIP). They further pointed out that monsoon zonal flow anomalies in the Indian Ocean can affect the sea-air interactions in the equatorial central and eastern Pacific through the GIP, triggering the occurrence of ENSO events [13]. Xu and Chan pointed out that the Asian-Australian monsoon system jointly affects the development of El Niño events, with a strong SASM and a strong East Asian winter monsoon being the necessary (but not sufficient) conditions. The El Niño phenomenon occurs when strong southerlies occur near the northeastern coast of Australia (and can converge with the northerlies associated with strong winter monsoons

Received 2019-10-12; **Revised** 2020-02-15; **Accepted** 2020-05-15

Funding: Strategic Priority Research Program of the Chinese Academy of Sciences (XDA20060503); Fund of Southern Marine Science and Engineering Guangdong Laboratory (ZJW-2019-08); National Key R&D Program of China (2017YFC1501802, 2018YFA0605604); Project of Enhancing School with Innovation of Guangdong Ocean University (230419053); Projects (Platforms) for Construction of Top-ranking Disciplines of Guangdong Ocean University (231419022)

Biography: YUAN Shuai, Master, primarily undertaking research on air-sea interaction and its effect on precipitation.

Corresponding author: XU Jian-jun, e-mail: jxu@gdou.edu.cn

in the Northern Hemisphere) [2]. Moreover, many studies have highlighted the role of El Niño events in the interannual variation of SASM (Boschat [14]; Pang and Yang [15]; Johnson et al. [16]). These works show that the Asian-Australian monsoon and ENSO events have formed an intricate atmosphere-ocean interaction system.

However, in spite of such a close relationship between the SASM and the ENSO cycle, a SASM anomaly does not always correspond to the occurrence of ENSO events (Xu and Chan [2]; Yun [17]). One possible explanation is that the SASM is mainly driven by the thermal contrast between the Asian landmass and adjacent oceans and exhibits only a significant regional feature. On the other hand, ENSO events are related to the planetary-scale circulation. Especially in recent years, some studies have shown that the relationship between ENSO and the South Asian summer monsoon has begun to weaken, and the South Asian summer monsoon itself is also weakening. Kumar analyzed the 140-year history record and found that the inverse correlation between ENSO and SASM weakened in the late 1970s [18]. With the development of satellite detection and models (Chang et al. [19]; Bollasina et al. [20]), many scholars have studied it from different perspectives (Lau [21]; Gershunov et al. [22]; Annamalai et al. [23]; Turner et al. [24]; Kucharski et al. [25]; Fan et al. [26]). Therefore, the main motivation of the present study is to examine further the relationship between the SASM and ENSO events and to identify possible mechanisms of their interaction.

Because the characteristics of the Asian summer monsoon vary widely from region to region, many indicators have been developed to describe the intensity and interannual variation of the monsoon (Shukla and Paolina [1]; Goswami et al. [27]; Wang and Fan [28]; Neng et al. [29]; Xu et al. [30]). Webster and Yang defined an index called Webster and Yang Index (WYI) based on the vertical shear of the zonal wind over the Asian monsoon region(0−20°N, 40ºE−100°E), which seems to describe the interannual variation of SASM well [6]. Using the optimal information extraction (OIE) method, Shi and Li reconstructed the SASM index based on 15 tree-ring chronologies [31]. On annual timescales, the generated index is significantly correlated with the South Asian summer monsoon index calculated using the instrument's records.

Xu and Chan used a technique proposed by Wiin-Nielsen [32] to break down the flow in the troposphere into the vertical mean flow and the shear flow, thus defining a South Asian summer monsoon index (SASMI) [33]. The results show that the SASMI can not only reflect the intensity of SASM well but also reflect some aspects of large-scale atmospheric circulation in the East Asian monsoon region. Therefore, the SASMI will be used in this study to define SASM intensity.

In section 2, the datasets used are described. The relationship between the South Asian summer monsoon and ENSO events is documented in Sections 3. Section 4 discusses the relationship between the South Asian summer monsoon and Walker circulations. The physical processes that may account for these relationships are examined in section 5. It will be summarized and discussed in Section 6.

2 DATA

The present study utilizes data from a number of sources. Monthly mean global zonal and meridional wind components as well as air temperature for 1958 through 2018 are from the NCEP / NCAR reanalysis (Kalnay et al. [34]). Monthly mean global SST data on a 2º latitude × 2º longitude grid from January 1958 to December 2018 are obtained from the NOAA Extended Reconstructed Sea Surface Temperature (SST) V5 (Huang et al. [35]). Monthly mean ocean heat content (0-2000m) data on a 1º latitude × 1º longitude grid for each month from January 1958 to December 2018 are from the IAP Gridded ocean subsurface temperature dataset (Cheng and Zhu [36]; Cheng et al. [37]). We used Niño 3.4 index to track ENSO, and the data come from the Climate Prediction Center (CPC).

3 RELATIONSHIP BETWEEN SASM AND ENSO CYCLE

3.1 *Shear kinetic energy and the South Asian summer monsoon*

Similar to the work of Xu and Chan [33], the horizontal wind (u, v) is divided into vertical mean (u_m, v_m) and vertical shear (u_s, v_s) values, which are the amount of deviation from the vertical average at each level. The shear kinetic energy [$K_s = (u_s^2 + v_s^2)/2$] in summer between June and August averaged over the period 1958−2018 shows two strong activity centers, one over the middle latitudes of the Asian landmass and the other over South Asia (Fig. 1). However, the time evolution of these two centers is different. The K_s in South Asia (boxed area in Fig. 1) increases significantly in mid-May, peaks in July and August, and then decreases in September (Fig. 2). This period corresponds to the active SASM. In contrast, mid-latitude K_s on the Asian continent are closely related to seasonal variations of planetary latitudinal winds in the Northern Hemisphere (NH), with the weakest in July and August and the strongest in December and January (Xu and Chan [33]).

Xu and Chan believed that K_s in South Asia should be a good indicator of SASM activities [33]. The average K_s in the region (0−20ºN, 40ºE−100ºE) from June to August is used as the South Asian summer monsoon index (SASMI), and the standard SASMI value can be calculated.

The interannual variation of the SASMI shows that between 1958−2018 there existed 16 strong monsoon episodes (standardized SASMI > 0.5): 1960, 1961, 1970, 1975, 1977, 1978, 1980, 1984, 1985, 1988, 1994, 1998,

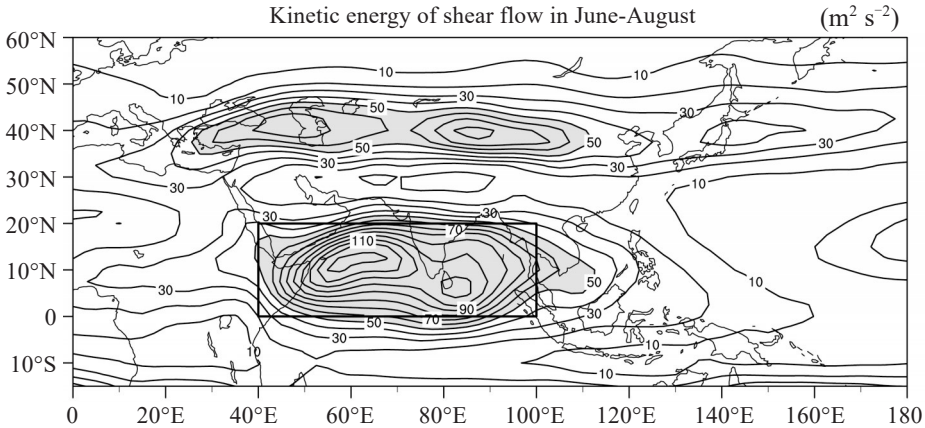

Figure 1. Kinetic energy of the vertical shear flow (K_s) averaged between June and August for the period of 1958−2018. Units: m^2 s^{-2}, contour interval 10 m^2 s^{-2}. Shading indicates values > 50 m^2 s^{-2}. The thick box indicates the area of South Asia.

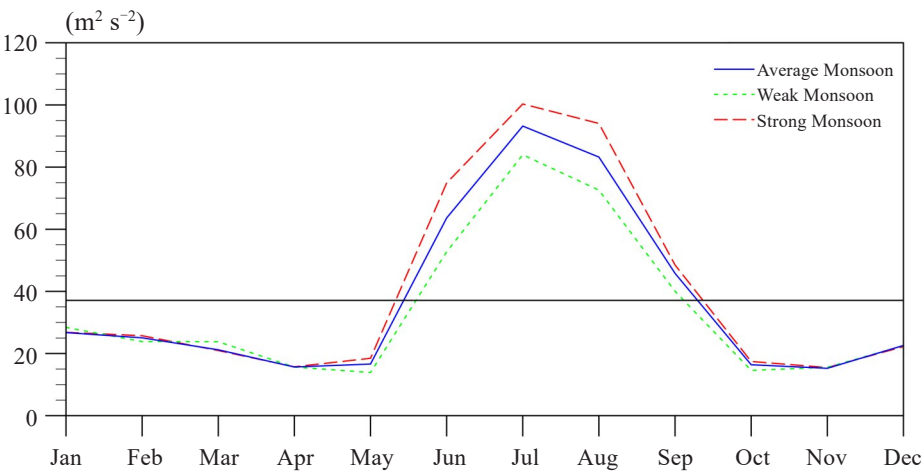

Figure 2. Monthly evolution of K_s averaged over South Asia (0−20ºN, 40ºE−100ºE) for strong monsoon episodes (dashed, red), weak monsoon episodes (dotted, green) and the average between 1958 and 2018 (solid, blue). The horizontal line (37 m^2 s^{-2}) is the annual average K_s for this 61-year period.

2001, 2006, 2017, 2018; and 16 weak monsoon episodes (standardized SASMI <− 0.5): 1962, 1963, 1965, 1972, 1974, 1979, 1983, 1987, 1989, 1992, 1993, 1997, 2002, 2009, 2011, 2015 (Fig. 3). Note that the SASMI shows a substantial interdecadal variation, but the interdecadal component will not be removed because the interdecadal variation trend is not consistent in different elements of the air-sea systems (Fig. 3).

The climatological annual mean (37 m^2 s^{-2}) of K_s over South Asia can be used as a threshold to define the onset (K_s > 37m^2 s^{-2}) and retreat (K_s < 37 m^2 s^{-2}) of the SASM. Based on this criterion, the average onset date of strong (weak) monsoon episodes is around May 10 (May 20) and the ending date is around September 15 (September 3). The persistent period is around 4 (3) months. It is clear that the strong monsoon episodes have not only a stronger intensity but also a longer duration (Fig.2).

3.2 *Relationship with ENSO events*

An El Niño event is identified if the 5-month running-average of the Niño 3.4 index exceeds 0.5 for 5 months or more. According to this method, if the index greater than 0.5 is interrupted for two months or more, the two events are considered to be discontinuous; if the interval is one month, and the 3-month moving average of the Niño 3.4 index for the month exceeds 0.5, it is considered that the front and back events are continuous, otherwise it is not continuous. Similarly, the Niño 3.4 index is less than −0.5 for La Niña events. From Fig. 3, it can also be seen that in the 19 El Niño years from 1958 to 2018, 8 events were in weak monsoon years, 8 in normal monsoon years and 3 in a strong monsoon year. In contrast, of the 19 La Niña years, 6 events were in strong monsoon years, 11 in normal monsoon years and 2 in a weak monsoon year. The relationship between SASM and ENSO can therefore be categorized into nine patterns: weak monsoon - El Niño (WM-EN), weak monsoon - non ENSO (WM-NE), weak monsoon - La Niña (WM-LN), normal monsoon - El Niño (NM-EN), normal monsoon - non ENSO (NM-NE), normal

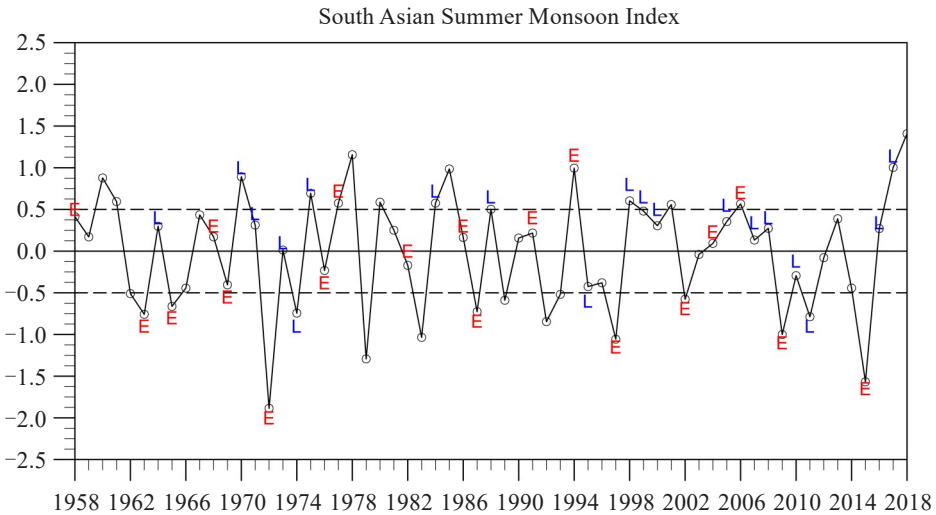

Figure 3. Interannual variation of the standardized South Asian summer monsoon index (SASMI) for the period of 1958−2018. "E"-El Niño years, "L"-La Niña years.

monsoon - La Niña (NM-LN), strong monsoon - El Niño (SM-EN), strong monsoon - non ENSO (SM-NE), and strong monsoon - La Niña (SM-LN).

Since the SM-EN and WM-LN patterns seldom occur and the NM-NE pattern is just the "normal" case, only the other six patterns will be examined in detail. These years are listed in Table 1.

Table 1. The years are listed according to the categories of the relationship between SASM and ENSO. The abbreviations are as follows: weak monsoon (WM), normal monsoon (NM), strong monsoon (SM), El Niño (EN), non ENSO (NE), and La Niña (LN).

Patterns	Years
WM-EN	1963, 1965, 1972, 1987, 1997, 2002, 2009, 2015
NM-EN	1958, 1968, 1969, 1976, 1982, 1986, 1991, 2004
WM-NE	1962, 1979, 1983, 1989, 1992, 1993
SM-LN	1970, 1975, 1984, 1988, 1998, 2017
NM-LN	1964, 1971, 1973, 1995, 1999, 2000, 2005, 2007, 2008, 2010, 2016
SM-NE	1960, 1961, 1978, 1980, 1985, 2001, 2018

Note that because ENSO events always mature during the winter, these patterns actually indicate the relationship between the previous SASM and following ENSO events.

4 THE RELATIONSHIP BETWEEN MONSOON CIRCULATION AND WALKER CIRCULATION

To understand the relationship between the SASM and ENSO events, the low-level (850hPa) and upper-level (200hPa) circulations are composited for each pattern averaged over the summer period (June - August).

4.1 *Low-level circulation*

For the WM-EN pattern (Fig. 4a), the tropical South Asian monsoon area (west of 100ºE) is dominated by easterly anomalies and anticyclonic flow is found over the Indian continent. Over the western North Pacific, westerly anomalies prevail over the equatorial area (east of 130ºE), and an Inter-Tropical Convergence Zone (ITCZ) appears around 15ºN. The center of anomalous subtropical high is located near 30ºN.

For the NM-EN pattern (Fig. 4b), the circulation anomalies over the western North Pacific is similar to that in the WM-EN pattern except for the intensity of the anomalous anticyclone. In contrast, the circulation over the South Asian monsoon area shows a different feature, with the westerly anomalies over the Bay of Bengal and the most part of the Indian continent.

For the WM-NE pattern (Fig. 4c), the circulation over the western Pacific is almost opposite to that in the above two patterns, with an easterly anomaly dominating over equatorial areas. Northeasterly anomalies prevail over the tropical South Asian monsoon area, which is linked to easterly anomalies over the western Pacific.

For the SM-LN pattern (Fig. 4d), the zonal wind over the South Asian monsoon areas and the equatorial Pacific are almost opposite to that in the WM-EN pattern (Fig. 4a). Similarly, the circulation over the areas

of Indo-China peninsula and the western North Pacific do show these opposite features. The results show that the correlated patterns of SASM and ENSO events exist not only in the tropics but also in the mid-latitudes. For the NM-LN pattern (Fig. 4e), the tropical circulation also shows an opposite feature to that in the NM-EN (Fig. 4b), some areas are not obvious but still exist over the middle latitudes. The circulation in the SM-NE pattern (Fig. 4f) also show the opposite feature to that in WM-NE pattern (Fig. 4c), although the location of the circulation anomalies is slightly different.

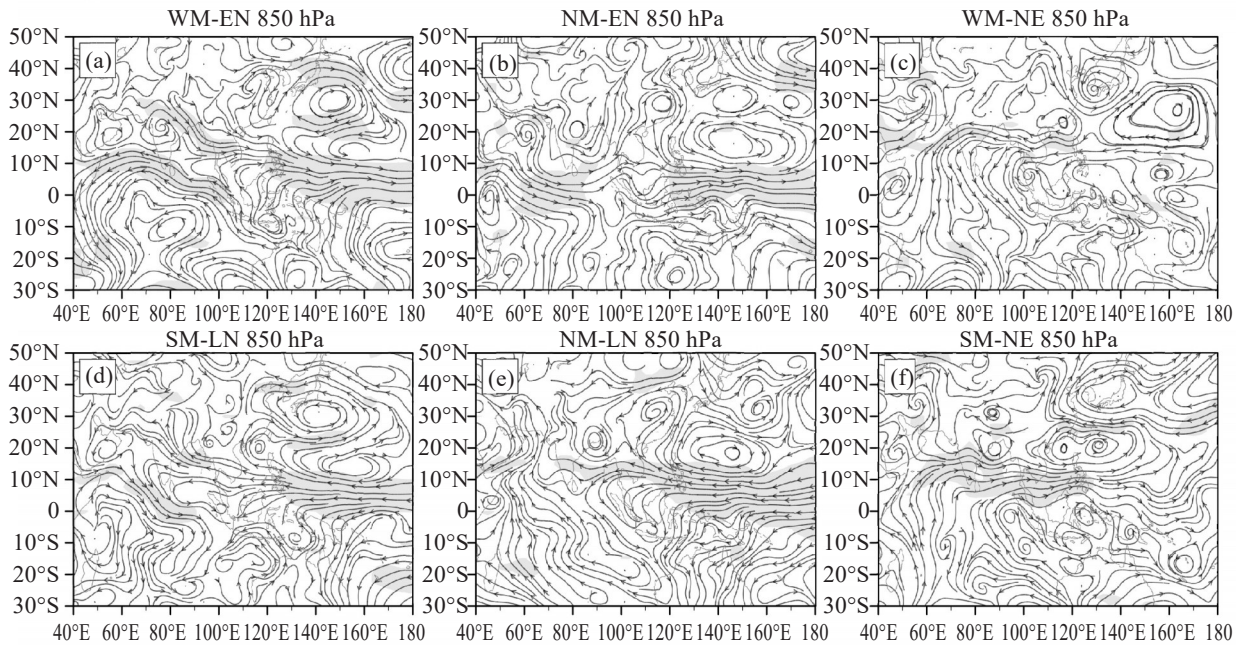

Figure 4. Composite 850hPa wind anomalies averaged between June and August in (a) weak monsoon-El Niño episodes (WM-EN), (b) normal monsoon-El Niño episodes (NM-EN), (c) weak monsoon-non ENSO episodes (WM-NE), (d) strong monsoon-La Niña episodes (SM-LN), (e) normal monsoon-La Niña episodes (NM-LN), and (f) strong monsoon-non ENSO episodes (SM-NE) years. The shaded areas indicate the *t* value in zonal wind anomalies exceeding significantly the confidence level of 0.10.

Based on the above results, we can find that the circulation anomalies are affected jointly by the monsoon and ENSO events. The corresponding anomalous patterns show opposite characteristics not only in the tropical areas but also in the middle latitude areas.

In addition, the statistical *t*-test shows (shaded areas in Fig. 4) that the circulation anomalies over the any key areas, including the South Asian monsoon area, western equatorial Pacific, exceed significantly the confidence level of 0.10, which means that the circulation anomalies pattern is reasonable. The following *t*-test in other fields also shows these features.

4.2 *Upper-level circulation*

At 200hPa, westerly anomalies dominate the entire tropical South Asian monsoon area in the WM-EN pattern (Fig. 5a), and easterly anomalies are found over the equatorial western Pacific, corresponding to westerly anomalies at the low-level (Fig. 4a). The circulation anomalies at the low and upper levels, therefore, suggest the existence of two vertical anomalous circulations: Asian monsoon vertical zonal circulation (hereinafter referred to as MC) over the tropical Indian Ocean and Walker circulation (WC) over the tropical Pacific.

For the NM-EN pattern (Fig.5b), easterly anomalies dominate over the tropical western Pacific and the South Asian monsoon area is also dominated by easterly anomalies. In contrast, the westerly anomalies occupy the entire tropical area from the South Asian monsoon area to the western Pacific in the WM-NE pattern (Fig. 5c). Similar to the low-level, the tropical circulation anomalies in the SM-LN (Fig. 5d) is opposite to that in the WM-EN pattern (Fig. 5a), which include the circulation anomalies over the middle latitudes. For the NM-LN (Fig. 5e) and NM-EN (Fig. 5b) patterns, the circulation anomalies also show negative correlation. The same is true for the SM-NE (Fig. 5f) and the WM-NE (Fig. 5c) patterns.

4.3 *Monsoon and Walker circulations*

Corresponding to the horizontal circulation at lower (Fig. 4) and upper (Fig. 5) circulation level, the velocity potential and divergence distribution on the lower level (850hPa) reflect the vertical motion (Fig. 6). For the WM-EN pattern, the South Asian monsoon area, and the regions from the Indo-China peninsula through the maritime continent as well as the northeastern ocean of Australia, are dominated by the divergence anomalies. The former area is consistent with the weak SASM, while the latter area implies that the descent anomalous motion dominates these areas, which is concomitant with the weak WC and weak MC. In contrast, the

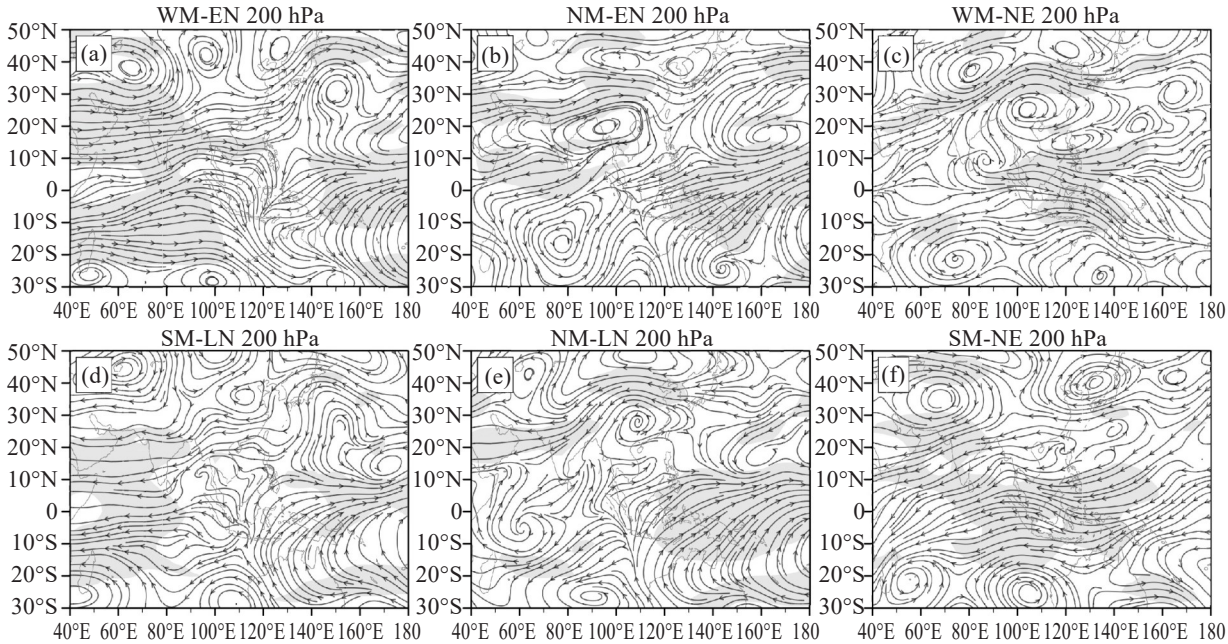

Figure 5. The same as Fig. 4 but for the 200hPa.

convergence anomalies dominate the South Asian monsoon area, the maritime continent and adjacent areas in the SM-LN pattern (Fig. 6d), which just reflect the effect of the strong SASM and La Niña events.

For the NM-EN pattern (Fig. 6b), the strong divergence is found over the maritime continent and surrounding areas, which still reflect the feature of the weak WC. In most of the South Asian monsoon region, the divergence value is small, which just shows that the SASM is normal. The divergence distribution over the western equatorial Pacific in the NM-LN pattern (Fig. 6e) shows an opposite feature to that in the NM-EN pattern (Fig. 6b). The divergence over the South Asian monsoon area also shows a weak anomaly.

For the WM-NE (Fig. 6c) patterns, the Asian landmass areas show divergence anomaly, while the SM-NE (Fig. 6f) shows convergence anomaly, which corresponds to weak and strong monsoon events. In contrast, the divergence over the western equatorial Pacific and the maritime continent indicate a weak anomaly, which reflects the normal state of the tropical Pacific. It can be seen that the ENSO event is the main driving force for vertical circulation anomalies.

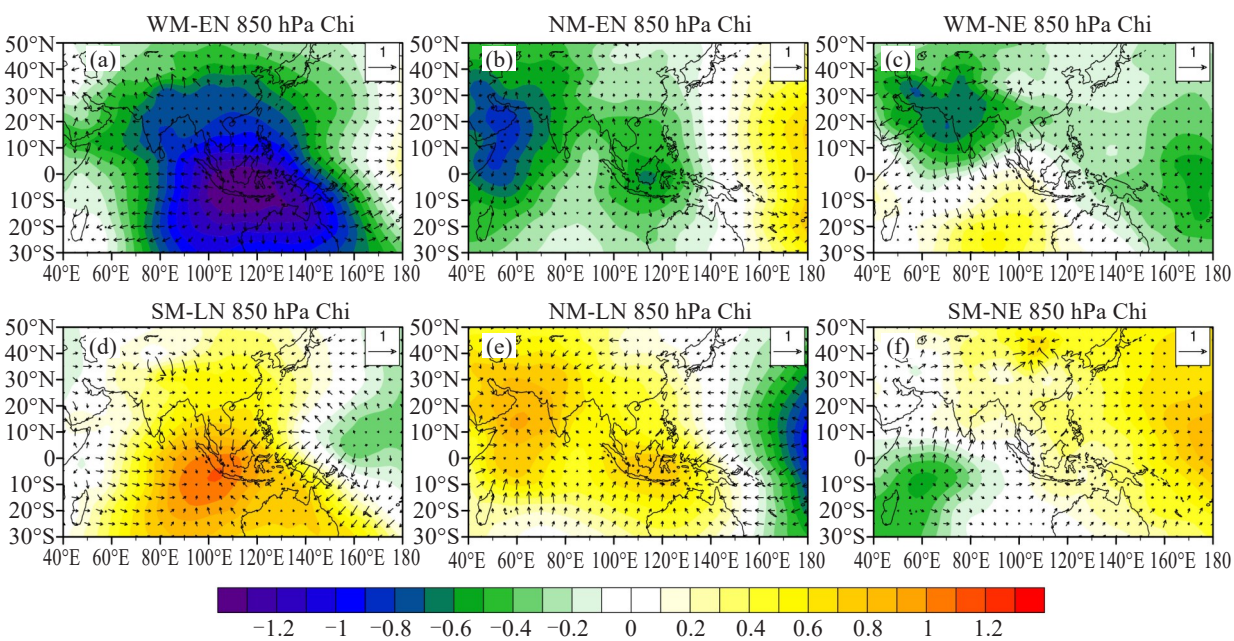

Figure 6. Composite 850hPa divergence wind and velocity potential anomalies averaged between June and August in (a) WM-EN, (b) NM-EN, (c) WM-NE, (d) SM-LN, (e) NM-LN, and (f) SM-NE years. The colour map represents the velocity potential (Chi scaled by 1e6), and the arrow represents the divergence wind.

Table 2. In the six classifications, the extreme values of the 850hPa velocity potential anomaly near the maritime continent (20°S−10°N, 90°E−120°E) are listed in the second column. The differences between the Walker circulation anomaly in the eastern region (190°W−230°W) and the western region (90°E−130°E) are listed in the third column.

Patterns	850 hPa Chi anomaly's extreme values	Vertical circulation difference
WM-EN	−1.464492	−1.454965
NM-EN	−0.6258565	−0.5513107
WM-NE	−0.3196093	0.2063123
SM-LN	1.11268	0.9231751
NM-LN	0.7951069	0.7670668
SM-NE	0.3632113	−0.1157316

The extreme values of the velocity potential anomaly in Table 2 represent its intensity, and the larger positive value indicates strong convergence here, and vice versa. Through analysis and graphical comparison, we can find that the anomalous values in WM-EN and SM-LN patterns are much larger than those of the other four groups (Table. 2). We call the strong coupled phenomenon of WM-EN and SM-LN the resonance effect. It can be seen that the anomalous values under the resonance effect are twice that of the non-monsoon patterns (NM-EN, and NM-LN) and 4−5 times that of the non-ENSO patterns (WM-NE, SM-NE). Under what conditions can resonance effects be produced? We will answer this question in the mechanism analysis section.

Based on the lower and upper horizontal circulations as well as the divergence wind and the velocity potential distribution, the MC and WC over the South Asian monsoon area and tropical Pacific can be summarized as the schematic diagram (Fig. 7). The feature can be summarized as follows:

- The WC associated with ENSO events is not always correlated with the MC associated with the SASM. The easterly (westerly) anomalies in weak (strong) SASM occurs while the westerly (easterly) anomalies over the tropical Pacific in El Niño (La Niña) (WM-EN, SM-LN), which only account for around 40% in ENSO events. For the NM-EN, WM-NE, NM-LN, and SM-NE patterns, the circulations over the South Asian monsoon area and the equatorial Pacific are uncorrelated.
- The relative intensity of the WC and MC is different and the cores of their maximum anomalous zonal wind do not locate at the same equatorial zone. The position of MC is always north of the equator (10ºN−15ºN).
- For the four uncorrelated patterns (NM-EN, WM-NE, NM-LN, SM-NE), the MC direction on the vertical section is often in the same direction in the WC, which means that the rising or subsidence branch of MC is different from that in the WC over the maritime continent and surrounding areas. These results indicate that the MC and WC are the two relative independent systems.

This result shows that the South Asian summer

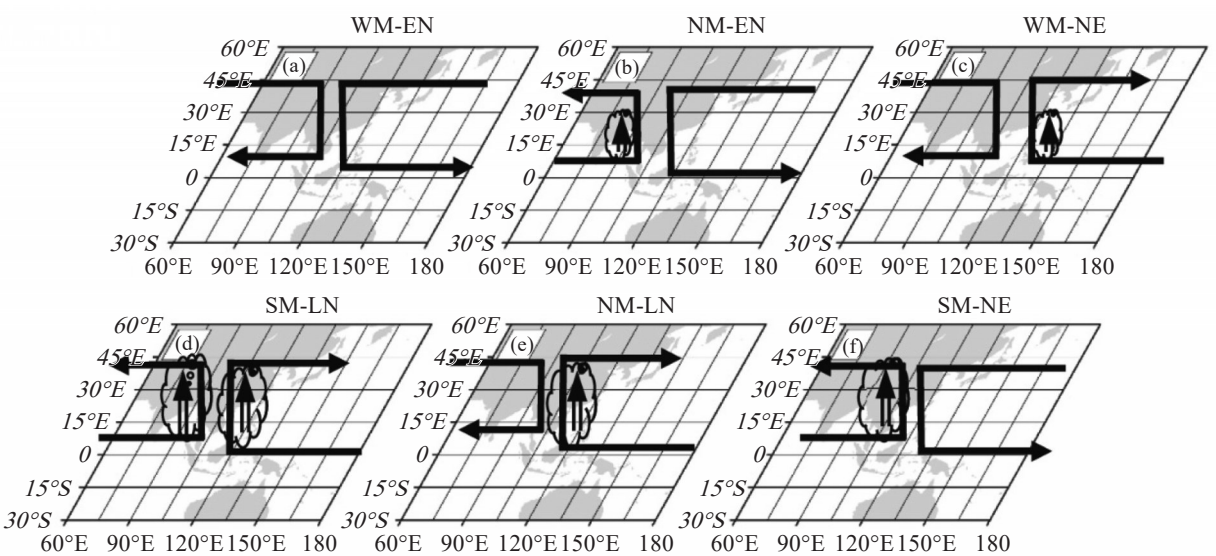

Figure 7. A schematic diagram illustrating the location of the South Asian summer monsoon zonal circulation (MC) and Walker circulation (WC) in (a) WM-EN, (b) NM-EN, (c) WM-NE, (d) SM-LN, (e) NM-LN, and (f) SM-NE. The arrow in the cloud and the size of the cloud represent the updraft and its intensity.

monsoon and ENSO are not always strongly correlated. Only when certain conditions are met can a strong coupling phenomenon occur, which is the resonance effect we have proposed. The mechanism for the present results will be discussed in the following sections.

5 THE PHYSICAL PROCESSES RESPONSIBLE FOR THE RELATIONSHIP BETWEEN THOSE TWO SYSTEMS

5.1 *Atmospheric processes*

5.1.1 MEAN TEMPERATURE ANOMALIES FROM 500HPA TO 200HPA

In order to reflect the thermal contrast over the Asia-Pacific areas, the mean temperature anomalies from 500hPa to 200hPa are composited. Concomitant with the weak SASM, the Asian landmass is dominated by the cold anomalies in the WM-EN pattern (Fig. 8a), and the entire tropical Indian Ocean shows a positive anomaly, which is similar to the sign in the tropical Pacific except for its large anomalous amplitude. This feature just reflects the effect of El Niño events. Obviously, the behavior is almost opposite in the SM-LN pattern (Fig. 8d); a warm anomaly is in Asian landmass and the negative anomalies in the tropical ocean with the maximum in the southern Pacific. The warming anomaly in the Asian landmass is greater than that in the Indian Ocean, and the resulting land-sea thermal gradient contributes to the development of a strong monsoon.

For the NM-EN pattern, a cold anomaly zone is found in the mid-high latitudes of the Asian continent (Fig. 8b). The tropical Indian Ocean also exhibits weak negative anomalies and forms a distinct temperature gradient with the tropical Pacific. It is clear that this distribution is beneficial to the formation of the pressure gradient, which produces westerly anomalies on the equatorial Pacific Ocean (Fig. 8b). The opposite distribution is also found in the NM-LN pattern (Fig. 8e). The tropical Indian Ocean is a weak positive anomaly, and the Asian continent is a positive anomaly. The anomalous symbols on the equatorial Pacific are opposite to them. It is easy to form an easterly anomaly on the equatorial Pacific Ocean.

In addition, the behavior in the following two patterns (Fig. 8c and f) shows a similar indication. We can see that due to the absence of ENSO events, the temperature anomaly is smaller in the Pacific region, while the comparison between the Asian continent and the Indian Ocean is more obvious. The change in the direction of temperature gradient corresponds to each pattern. For example, when the monsoon is strong, the wind generally blows from the ocean to the land.

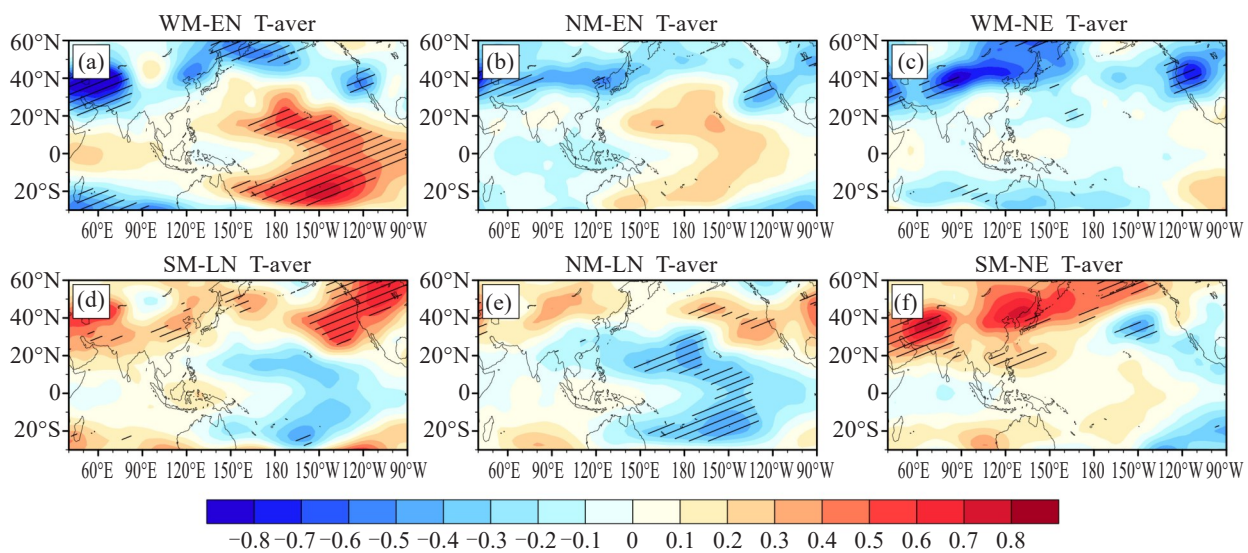

Figure 8. Composite air temperature anomalies from 500hPa to 200hPa averaged between June and August in (a) WM-EN, (b) NM-EN, (c) WM-NE, (d) SM-LN, (e) NM-LN, and (f) SM-NE years. Shading indicates that the *t* value of composite anomalies exceeds significantly the confidence level of 0.10.

In the resonance patterns (Fig. 8a and 8d), we can find that the main factor for the resonance effect is the phenomenon that the symbols of SSTA in the tropical Indian Ocean and the equatorial eastern Pacific are the same, but are opposite to that of the SSTA near the maritime continent. The SSTA of other non-resonant patterns do not satisfy this condition.

5.1.2 VERTICAL CIRCULATION

The distribution of zonal circulation shows a substantial difference over three key areas: the equatorial central-eastern Pacific, the tropical Indian Ocean, and the maritime continent. For the WM-EN pattern (Fig. 9a), due to warming in the equatorial central-eastern Pacific, equatorial convection and the ascending branch of the Walker circulation, normally located in the western Pacific, anomalously move eastward, resulting in an abnormal sinking zone from Indo-China peninsula through the maritime continent as well as the

northeastern ocean of Australia (corresponding to Fig. 6a). The behavior is just opposite in the SM-LN pattern (Fig. 9d). The updrafts in the West Pacific and the maritime continent enhance the Walker circulation and monsoon circulation, which is conducive to the development of strong monsoon. From the vertical circulation diagrams of the two patterns (Fig. 9a and b), we can see that there are two relatively clear zonal circulation loops, which are the MC and the WC we mentioned above.

For the NM-EN pattern and the NM-LN pattern (Fig. 9b and e), the Walker circulation is still quite obvious due to ENSO events. However, the difference is that the monsoon circulation is in the same direction as the Walker circulation in the vertical plane. For example, in Fig. 9b, both circulation anomalies are counterclockwise. However, due to non-monsoon events, the circulation pattern is less obvious in the Indian Ocean region.

For the WM-NE pattern and the SM-NE pattern (Fig. 9c and f), there is no ENSO event, so the Walker circulation is not obvious. However, it can be seen that there is abnormal updraft in the tropical Indian Ocean in Fig. 9c, which indicates that the temperature increases and the resulting thermal differences between land and sea tend to form weak monsoons. The behavior is just opposite in the SM-NE pattern (Fig. 9f).

In order to quantitatively show the strength of the circulation, we selected two regions of the vertical velocity difference between the eastern region (90° E−130° E) and the western region (190° W−230° W) to compare the changes in the circulation. The specific values are also shown in Table 2. We can see that the difference of the resonance patterns are still the largest, and the non-ENSO patterns are the smallest, corresponding to the velocity potential anomalies in the previous column.

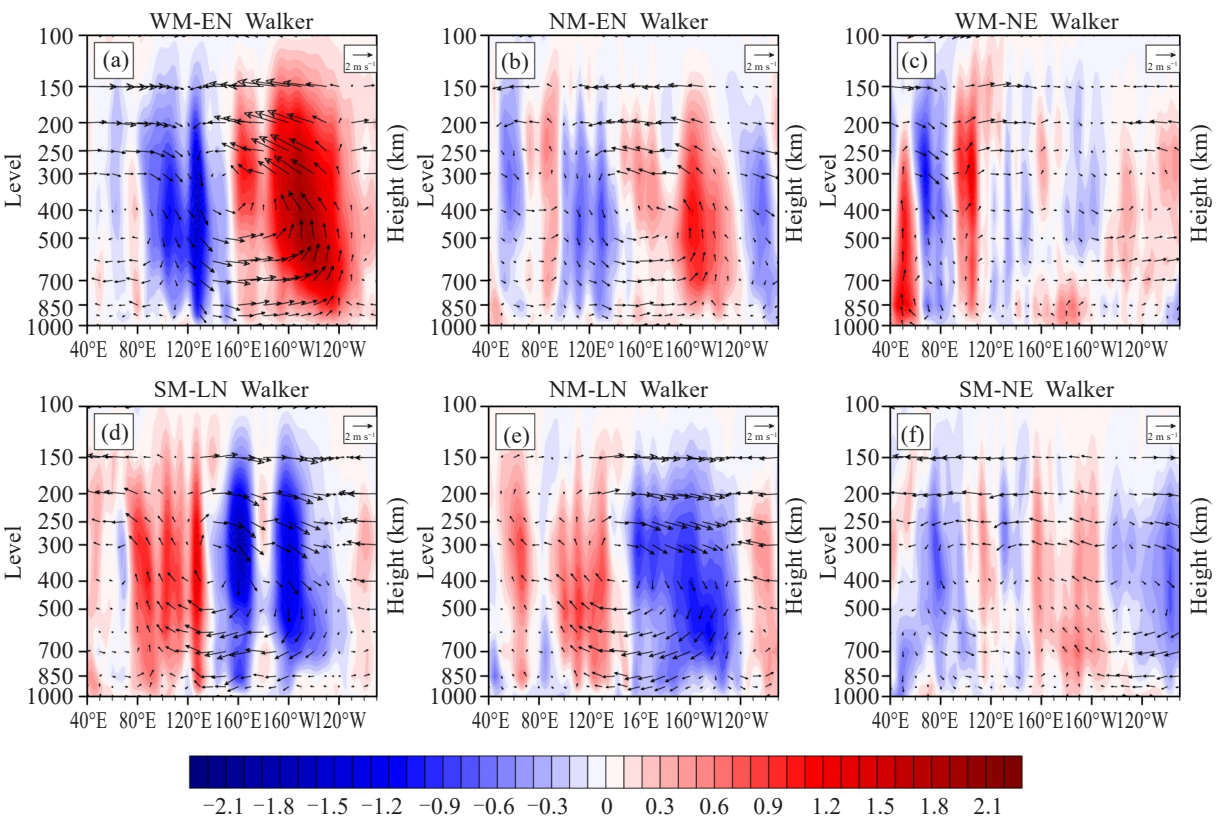

Figure 9. Composite zonal circulation(10° S−10° N) anomalies averaged between June and August in (a) WM-EN, (b)NM-EN, (c) WM-NE, (d) SM-LN, (e) NM-LN, and (f) SM-NE years. The coloring areas represent the vertical wind anomalies (omega*-100) and the arrows indicate a combination of zonal and vertical wind anomalies.

5.2 *Oceanic processes*

5.2.1 SEA SURFACE TEMPERATURE

For the WM-EN pattern, associated with the El Niño episodes, the sea surface temperature (SST) over the eastern equatorial Pacific (EEP) shows a positive anomaly (Fig. 10a), and is positively correlated with the counterpart over the tropical Indian Ocean, which is favorable for the air temperature rising above there (Fig. 8a). Similarly, when the strong monsoon years correspond to the La Niña episodes (Fig. 10d), both the tropical Indian Ocean and the EEP are dominated by negative anomalies. Obviously, in these two resonance patterns, the SST near the western equatorial Pacific Ocean, which is close to the oceanic continent, is negatively correlated with the SSTA in these two places.

In contrast, in the NM-EN pattern (Fig. 10b), most

of the tropical Indian Ocean is replaced by the negative anomaly, which attenuates the temperature rising in the region, while EEP is still occupied by warm temperature anomalies. For the NM-LN pattern (Fig. 10e), the SSTA over the tropical Indian Ocean is basically negatively correlated with EEP.

Since there is no ENSO episodes in the WM-NE (Fig. 10c) and the SM-NE (Fig. 10f) pattern, the weak SSTA appeared over the tropical ocean.

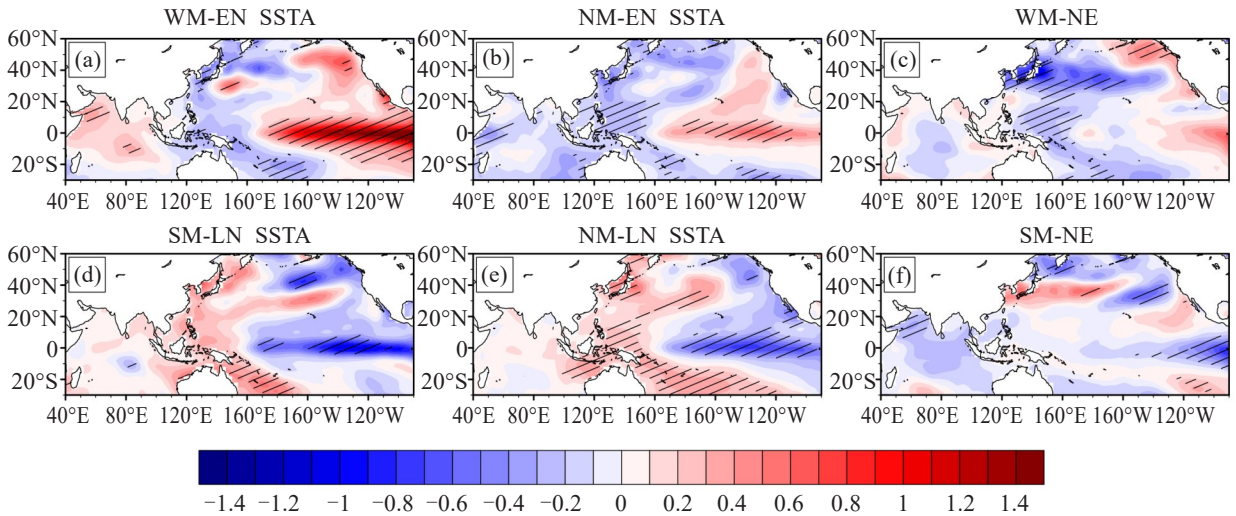

Figure 10. Composite sea surface temperature anomalies (SSTA) averaged between June and August in (a) WM-EN, (b) NM-EN, (c) WM-NE, (d) SM-LN, (e) NM-LN, and (f) SM-NE years. Shading indicates that the *t* value of composite anomalies exceeds significantly the confidence level of 0.10.

5.2.2 OCEANIC HEAT CONTENT

In addition to SSTA, ENSO events are also related to the subsurface ocean temperature anomalies. To explore how these anomalies relate to the six patterns, the composite of sub-surface heat content anomalies (HCAs) from 0 to 400 m depth is selected for analysis. In the WM-EN pattern, positive HCAs are found in the tropical Indian Ocean and the EEP (Fig. 11a), most part of which corresponds to the positive SSTA (see Fig. 10a). This contributes the warm SSTA over there. The behavior is opposite in the SM-LN pattern (Fig. 11d).

In the NM-EN (NM-LN) pattern (Figs. 11b, e), HCAs show negative (positive) values in most parts of the tropical Indian Ocean, as opposed to HCAs in EEP. In addition, the HCAs also seem to be very weak in the WM-NE and SM-NE patterns (Fig. 11c and f).

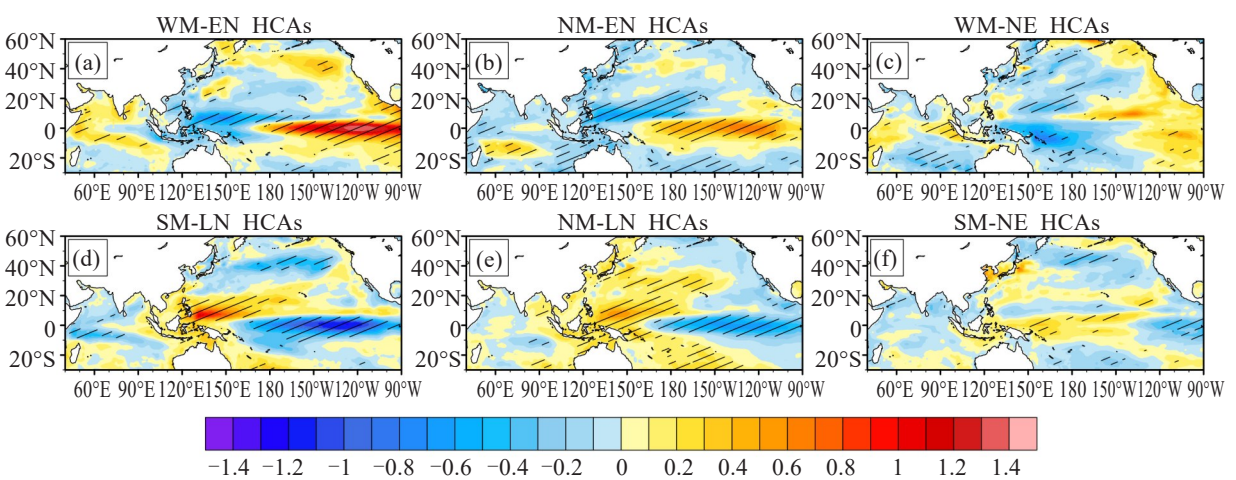

Figure 11. Composite oceanic heat content anomalies (HCAs) from 0 to 400 m depth averaged between June and August in (a) WM-EN, (b)NM-EN, (c) WM-NE, (d) SM-LN, (e) NM-LN, and (f) SM-NE years. Shading indicates that the *t* value of composite anomalies exceeding significantly the confidence level of 0.10.

Through the comparison of ocean heat content anomaly and SST anomaly, it can be seen that there is a good correspondence between them, with their anomalous area being the same. This also shows that the change of sea surface temperature is closely related to the ocean heat content. However, by comparing the temperature anomalies with the sea surface anomalies, we can see that the WM-NE and SM-NE patterns do not

exactly match (Fig. 8c and f, and Fig. 10c and f). This indicates that although sea surface temperature anomalies affect temperature anomalies to some extent through air-sea interactions, there are other influencing factors.

5.3 *A hypothesis*

Based on the differences in various parameters currently analyzed so far, it is possible to propose a hypothesis to describe the sequence of physical processes, thereby explaining for the relationship between SASM anomalies and ENSO events. From the perspective of the atmosphere, those two vertical cells MC and WC associated with the SASM and ENSO events are not always consistent with the findings (Barnett [38]; Yasunari [39]) that the strong (weak) westerly over Asian monsoon area was accompanied by the strong (weak) trade over the tropical Pacific (Figs. 4 and 7). The uncorrelated circulation is mainly from different physical processes. The MC is controlled by thermal gradients between the Asian landmass and the tropical Indian Ocean, whereas the WC associated with ENSO events is primarily the east-west thermal gradient between the tropical South Pacific and the tropical Indian Ocean. Furthermore, the gradient directions caused by different surface thermal conditions are different (Fig. 8). In general, the change of thermal status over Asian land is not just consistent with its counterpart over the tropical ocean. In fact, the MC is related to the WC only when the signal of change over the eastern equatorial Pacific (EEP) is the same as that over the tropical Indian Ocean and the signal of change over the Asian continent is the opposite (See Fig. 8a and d). However, the thermal condition over the Asian continent and the Indian-Pacific Ocean does not always change with this pattern, so the changes in the Asian summer monsoon are not associated with the ENSO events most of the time.

Ocean thermal conditions, on the other hand, alter the pressure gradient and thus modulate the relative temperature distribution. The main reason is the sign of SSTA over the tropical Indian-Pacific Ocean. Usually, the SST change over the tropical Indian Ocean is at the same sign as that in the EEP (Fig. 10a and d), which is conducive to the correlation between the SASM and ENSO episodes. However, it is not always the case. In many cases, the SST variation over the tropical Indian Ocean is not completely consistent with that over the eastern equatorial Pacific (Fig. 10b and e), which is similar to conclusions of previous work (Nicholls [40]; Webster et al. [41]; Saji et al. [42]). Therefore, the SASM is not always related to ENSO events. Of course, the different variation of SST over the Indian Ocean and Pacific is from the different ocean circulation and the different sub-surface condition (See Fig. 11).

In short, the MC is a relatively independent system from the WC. The different surface thermal conditions determine the different pressure gradient and modulate the relationship between the SASM and ENSO events.

6 SUMMARY AND DISCUSSION

6.1 *Summary*

According to Xu and Chan's work [33], the kinetic energy (K_s) shear component on the box (0−20ºN, 40º−100ºE) is defined as the South Asian summer monsoon index (SASMI), which is used to measure the intensity of the South Asian summer monsoon (SASM). By this index, the SASM can be divided into strong and weak monsoon episodes. In the past 61 years from 1958 to 2018, there existed 16 (16) strong (weak) monsoon episodes. Composite analysis shows that the strong monsoon episodes have not only a stronger intensity but also a longer persistent time.

The relationship between the South Asian summer monsoon anomalous episodes and the ENSO episodes can be categorized into six patterns: weak monsoon - El Niño (WM-EN), normal monsoon - El Niño (NM-EN), weak monsoon - non ENSO (WM-NE), strong monsoon - La Niña (SM-LN), normal monsoon - La Niña (NM-LN) and strong monsoon - non ENSO (SM-NE).

The WC associated with ENSO episodes is not always correlated to the MC associated with monsoon episodes. The easterly (westerly) anomalies in weak (strong) monsoon episodes occurs while the westerly (easterly) anomalies over the tropical Pacific in El Niño (La Niña) episodes (WM-EN, SM-LN), which account for around 40% of ENSO events. The relative intensity of the WC and MC is different and the cores of their maximum anomalous zonal wind do not locate at the same equatorial zone. The position of MC is always at the north of the equator (~10ºN).

The mechanisms responsible for the MC and WC are different. The MC is controlled by the south-north thermal gradient between the Asian landmass and the tropical Indian Ocean, and the WC is dominated by the east-west thermal gradient between the southern pacific and tropical Indian Ocean. Furthermore, the gradient directions caused by different surface thermal conditions are different. In addition, we refer to the two strong coupled patterns WM-EN and SM-LN as resonance effects. The opposite sign of SSTA over the tropical Indian Ocean and the eastern equatorial Pacific is an important factor for the non-resonant patterns between the SASM and ENSO events.

6.2 *Discussion*

The present study suggests that the South Asian summer monsoon anomalies are different episodes from the ENSO episodes, and emphasizes that the strong (weak) South Asian summer monsoon episodes are not always consistent with the La Niña (El Niño). The main reason is from the different mechanism responsible for formation of monsoon and Walker circulations.

Many previous works pointed out that the Asian monsoon is closely related to ENSO episodes (Webster and Yang [6]; Yasunari [39]; Wu et al. [43]), and they even

found that monsoon zonal circulation over the tropical equatorial Indian Ocean and the Walker circulation over the Pacific is correlated (Wu and Meng [13]). However, the results of the present study implied that the monsoon zonal circulation is a relatively independent system from the Walker circulation associated with ENSO episodes. The relationship between the two strong signs is limited, which is determined by the surface thermal condition.

Although the variation of SASM has a good correlation with the ENSO episodes, the mechanisms for the two systems are different substantially; in particular, the correlation between the monsoon and ENSO has weakened in recent decades. Should we consider SASM anomalies as relatively independent events? These results give us a clue that the weather or climate change, especially that over the monsoon areas, is not always from ENSO anomalies over the Pacific and is perhaps from monsoon anomalies. Over the Ocean, why are not the SSTA over the eastern equatorial Pacific consistent with that over the tropical Indian Ocean at some point? How do the SASM and ENSO events work together to affect climate change in Asia? In addition, we also propose a resonance effect between the monsoon and ENSO. When this effect occurs, how does it affect the global climate? Besides the thermal condition, is there any dynamic mechanism for the occurrence of this resonance effect? These questions will be discussed as the main topic of our next article.

***Acknowledgments*:** We thank the ESRL, IAP, NOAA and CPC for the availability of the data used in this work. The data used in the study are available at https://www.esrl.noaa.gov/psd/data/gridded / data. ncep. reanalysis. pressure. html, http://159.226.119.60 / cheng/, https://www. esrl. noaa. gov / psd / data / gridded/data.noaa.ersst.v5.html and https://www.cpc.ncep.noaa.gov / products / analysis_monitoring / ensostuff / detrend. nino34. ascii.txt.

REFERENCES

[1] SHUKLA J, PAOLINO D A. The Southern Oscillation and long-range forecasting of the summer monsoon rainfall over India [J]. Mon Wea Rev, 1983, 111(9): 1830-1837, https://doi. org / 10.1175 / 1520-0493(1983)111<1830: TSOALR>2.0.CO;2.

[2] XU J, CHAN J C. The role of the Asian-Australian monsoon system in the onset time of El Niño events [J]. J Climate, 2001, 14(3): 418-433, https://doi. org / 10.1175 / 1520-0442(2001)014<0418:TROTAA>2.0.CO;2.

[3] RAJEEVAN M, MCPHADEN M J. Tropical Pacific upper ocean heat content variations and Indian summer monsoon rainfall [J]. Geophys Res Lett, 2004, 31(18): L18203, https: //doi.org/10.1029/2004GL020631

[4] SOMAN M, SLINGO J. Sensitivity of the Asian summer monsoon to aspects of sea - surface - temperature anomalies in the tropical Pacific Ocean [J]. Quart J Roy Meteorol Soc, 1997, 123(538): 309-336, https://doi. org / 10.1002 / qj.49712353804.

[5] SHI F, FANG K, XU C, et al. Interannual to centennial variability of the South Asian summer monsoon over the past millennium [J]. Climate Dynamics, 2017, 49(7-8): 2803-2814, https://doi.org/10.1007/s00382-016-3493-9.

[6] WEBSTER P J, YANG S. Monsoon and ENSO: Selectively interactive systems [J]. Quart J Roy Meteorol Soc, 1992, 118(507): 877-926, https://doi. org / 10.1002 / qj.49711850705.

[7] MEEHL G A. The south Asian monsoon and the tropospheric biennial oscillation [J]. J Climate, 1997, 10 (8): 1921-1943, https://doi. org / 10.1175 / 1520-0442(1997) 010<1921:TSAMAT>2.0.CO;2.

[8] LAU K M, YANG S. The Asian monsoon and predictability of the tropical ocean-atmosphere system [J]. Quart J Roy Meteorol Soc, 1996, 122(532): 945-957, https://doi. org / 10.1002/qj.49712253208.

[9] KIRTMAN B P, SHUKLA J. Influence of the Indian summer monsoon on ENSO [J]. Quart J Roy Meteorol Soc, 2000, 126(562): 213-239, https://doi. org / 10.1002 / qj.49712656211.

[10] KIM K M, LAU K M. Dynamics of monsoon - induced biennial variability in ENSO [J]. Geophys Res Lett, 2001, 28(2): 315-318, https://doi. org / 10.1029 / 2000GL012465.

[11] WU R, KIRTMAN B P. On the impacts of the Indian summer monsoon on ENSO in a coupled GCM [J]. Quart J Roy Meteorol Soc, 2003, 129(595): 3439-3468, https:// doi.org/10.1256/qj.02.214.

[12] LI Y, LU R, DONG B. The ENSO-Asian monsoon interaction in a coupled ocean-atmosphere GCM [J]. J Climate, 2007, 20(20): 5164-5177, https://doi. org / 10.1175/JCLI4289.1.

[13] WU Guo-xiong, MENG Wen. Gearing between the Indo-monsoon Circulation and the Pacific-Walker Circulation and the ENSO, Part I: Data analyses [J]. Scientia Atmospherica Sinica, 1998, 22(4): 470-480 (in Chinese).

[14] BOSCHAT G. Interannual Variability and Predictability of the Indian Summer Monsoon-El Niño Southern Oscillation System [D]. Paris: Université Pierre et Marie Curie-Paris VI, 2012.

[15] HSU P C, YANG Y. Contribution of atmospheric internal processes to the interannual variability of the south Asian summer monsoon [J]. International J Climatol, 2016, 36 (8): 2917-2930, https://doi.org/10.1002/joc.4528.

[16] JOHNSON S J, TURNER A, WOOLNOUGH S, et al. An assessment of Indian monsoon seasonal forecasts and mechanisms underlying monsoon interannual variability in the Met Office GloSea5-GC2 system [J]. Climate Dyn, 2017, 48(5-6): 1447-1465, https://doi.org/10.1007/s00382-016-3151-2.

[17] YUN K S, TIMMERMANN A. Decadal monsoon - ENSO relationships re-examined [J]. Geophys Res Lett, 2018, 45 (4): 2014-2021, https://doi.org/10.1002/2017GL076912.

[18] KUMAR K K, RAJAGOPALAN B, CANE M A. On the weakening relationship between the Indian monsoon and ENSO [J]. Science, 1999, 284(5423): 2156-2159, https:// doi.org/ 10.1126/science.284.5423.2156.

[19] CHANG S, ZHENG S, DU H, et al. A channel selection method for hyperspectral atmospheric infrared sounders based on layering [J]. Atmos Measurement Techniques, 2020, 13(2): 629-644, https://doi.org/10.5194/amt-13-629-2020.

[20] BOLLASINA M A, MING Y, RAMASWAMY V. Anthropogenic aerosols and the weakening of the south

Asian summer monsoon [J]. Science, 2011, 334(6055): 502-505, https://doi.org/10.1126/science.1204994.
[21] LAU K, EINAUDI F. Monsoon-Enso Relationships: A New Paradigm [D]. São Paulo: University of São Paulo, 2000.
[22] GERSHUNOV A, SCHNEIDER N, BARNETT T. Low-frequency modulation of the ENSO-Indian monsoon rainfall relationship: Signal or noise? [J]. J Climate, 2001, 14(11): 2486-2492, https://doi. org / 10.1175 / 1520-0442 (2001)014<2486:LFMOTE>2.0.CO;2.
[23] ANNAMALAI H, HAMILTON K, SPERBER K R. The South Asian summer monsoon and its relationship with ENSO in the IPCC AR4 simulations [J]. J Climate, 2007, 20(6): 1071-1092, https://doi.org/10.1175/JCLI4035.1.
[24] TURNER A, INNESS P, SLINGO J. The effect of doubled CO2 and model basic state biases on the monsoon - ENSO system, I: Mean response and interannual variability [J]. Quart J Royal Meteorol Soc, 2007, 133(626): 1143-1157, https://doi.org/10.1002/qj.82.
[25] KUCHARSKI F, BRACCO A, YOO J, et al. Low-frequency variability of the Indian monsoon-ENSO relationship and the tropical Atlantic: The "weakening" of the 1980s and 1990s [J]. J Climate, 2007, 20(16): 4255-4266, https://doi.org/10.1175/JCLI4254.1.
[26] FAN F, DONG X, FANG X, et al. Revisiting the relationship between the South Asian summer monsoon drought and El Niño warming pattern [J]. Atmos Sci Lett, 2017, 18(4): 175-182, https://doi.org/10.1002/asl.740.
[27] GOSWAMI B, KRISHNAMURTHY V, ANNMALAI H. A broad - scale circulation index for the interannual variability of the Indian summer monsoon [J]. Quart J Roy Meteorol Soc, 1999, 125(554): 611-633, https://doi. org/10.1002/qj.49712555412.
[28] WANG B, FAN Z. Choice of South Asian summer monsoon indices [J]. Bull Amer Meteorol Soc, 1999, 80 (4): 629-638, https://doi.org/10.1175/1520-0477(1999)080 <0629:COSASM>2.0.CO;2.
[29] SHI Neng, GU Jun-qiang, YI Yan-ming, et al. An improved south Asian summer monsoon index with Monte Carlo test [J]. Chin Physics, 2005, 14(4): 844, https://doi.org/10.1088/1009-1963/14/4/037.
[30] XU Z, FU C, QIAN Y. A new index to describe the tropical Asian summer monsoon [J]. Sci China Series D: Earth Sciences, 2009, 52(6): 843-854, https://doi. org / 10.1007/s11430-009-0058-3.
[31] SHI F, LI J, WILSON R J. A tree-ring reconstruction of the South Asian summer monsoon index over the past millennium [J]. Scientific Reports, 2014, 4: 6739, https:// doi.org/10.1038/srep06739.
[32] WIIN-NIELSEN A. On transformation of kinetic energy between the vertical shear flow and the vertical mean flow in the atmosphere [J]. Mon Wea Rev, 1962, 90(8): 311-323, https://doi. org / 10.1175 / 1520-0493(1962)090< 0311:OTOKEB>2.0.CO;2.
[33] XU J, CHAN J C. Relationship between the planetary - scale circulation over East Asia and the intensity of the South Asian Summer Monsoon [J]. Geophys Res Lett, 2002, 29(18): 131-134, https://doi. org / 10.1029 / 2002GL014918.
[34] KALNAY E, KANAMITSU M, KISTLER R, et al. The NCEP / NCAR 40-year reanalysis project [J]. Bull Amer Meteorol Soc, 1996, 77(3): 437-472, https://doi. org / 10.1175/1520-0477(1996)077<0437:TNYRP>2.0.CO;2.
[35] HUANG B, THORNE P, BANZON V, et al. NOAA Extended Reconstructed Sea Surface Temperature (ERSST) v5 [Z]. NOAA National Centers for Environmental Information, 2017.
[36] CHENG L, ZHU J. Benefits of CMIP5 multimodel ensemble in reconstructing historical ocean subsurface temperature variations [J]. J Climate, 2016, 29(15): 5393-5416, https://doi.org/10.1175/JCLI-D-15-0730.1.
[37] CHENG L, TRENBERTH K E, FASULLO J, et al. Improved estimates of ocean heat content from 1960 to 2015 [J]. Sci Adv, 2017, 3(3): e1601545, https://doi. org/ 10.1126/sciadv.1601545.
[38] BARNETT T. Interaction of the monsoon and Pacific trade wind system at interannual time scales, Part I: The equatorial zone [J]. Mon Wea Rev, 1983, 111(4): 756-773, https://doi. org / 10.1175 / 1520-0493(1983)111<0756: IOTMAP>2.0.CO;2.
[39] YASUNARI T. Impact of Indian monsoon on the coupled atmosphere / ocean system in the tropical Pacific [J]. Meteor Atmos Phys, 1990, 44(1-4): 29-41, https://doi.org/ 10.1007/BF01026809.
[40] NICHOLLS N. All-India summer monsoon rainfall and sea surface temperatures around northern Australia and Indonesia [J]. J Climate, 1995, 8(5): 1463-1467, https:// doi. org / 10.1175 / 1520-0442(1995)008<1463: AISMRA> 2.0.CO;2.
[41] WEBSTER P J, MOORE A M, LOSCHNIGG J P, et al. Coupled ocean-atmosphere dynamics in the Indian Ocean during 1997-98 [J]. Nature, 1999, 401(6751): 356-360, https://doi.org/10.1038/43848.
[42] SAJI N, GOSWAMI B, VINAYACHANDRAN P, et al. A dipole mode in the tropical Indian Ocean [J]. Nature, 1999, 401(6751): 360-363, https://doi.org/10.1038/43854.
[43] WU R, CHEN J, CHEN W. Different types of ENSO influences on the Indian summer monsoon variability [J]. J Climate, 2012, 25(3): 903-920, https://doi. org / 10.1175/ JCLI-D-11-00039.1.

Citation: YUAN Shuai, XU Jian-jun, CHAN J C L, et al. Resonance effect in interaction between South Asian Summer Monsoon and ENSO during 1958−2018 [J]. J Trop Meteor, 2020, 26(2): 137-149, https://doi.org/10.46267/j.1006-8775.2020.013.